JOURNAL OF SOLID STATE CHEMISTRY 37, 294–301 (1981)

Phase Equilibria and Compound Formation in the Nd–Mo–O System between 1273 and 1673°K

H. CZESKLEBA-KERNER,* B. CROS, AND G. TOURNE

Laboratoire de Chimie des Solides, Université des Sciences et Techniques du Languedoc, Place Eugène Bataillon, 34060 Montpellier Cédex, France

Received June 23, 1980; in final form September 10, 1980

Phase equilibria in the Nd_2O_3–MoO_2–MoO_3 system have been investigated at 1273, 1473, and 1673°K under a controlled gaseous atmosphere with emphasis on the formation and stability of ternary phases. New fluorite-related compounds of molybdenum VI and V have been characterized: Nd_6MoO_{12}, $Nd_{10}Mo_2O_{21}$, and Nd_3MoO_7. In the MoO_2-rich portion of the phase diagram a new cubic-related molybdenum IV compound, $Nd_2Mo_3O_9$, has been found. On the basis of phase equilibria at 1473°K, the standard free energies of formation of Nd_2MoO_5, Nd_3MoO_7, Nd_6MoO_{12}, and Nd_2MoO_6 were determined from metallic molybdenum, Nd_2O_3, and oxygen. The role of the rare earth element in selective oxidation of molybdenum and crystal chemical properties of the ternary compounds is discussed in relationship to the neighboring systems of praseodymium and samarium oxides.

Introduction

In previous work it has been shown that the oxidation states IV, V, and VI of molybdenum in mixed rare earth oxides are strongly stabilized against reduction through the rare earth element (*1*, *2*). Investigation of several rare earth–molybdenum–oxygen systems indicates that molybdenum can be selectively oxidized by fixing the oxygen partial pressure and choosing the rare earth element (*3*). In the present study phase equilibria in the Nd_2O_3–MoO_2–MoO_3 system have been established between 1273 and 1673°K under varying oxygen partial pressure ranging from 10^{-5} to 10^{-14} atm.

On the pseudobinary line Nd_2O_3–MoO_3, the following new fluorite-type compounds were identified as stable phases for $Nd_2O_3/Mo = 3/1, 5/2$: Nd_6MoO_{12} and $Nd_{10}Mo_2O_{21}$. Two new molybdenum V compounds have been characterized for the ratio $Nd_2O_3/Mo = 3/2, 1/2$: Nd_3MoO_7 and $NdMoO_4$. In the molybdenum-rich portion of the phase diagram, two compounds have been found for the molar ratio $Nd_2O_3/Mo = 1/2$ and $1/3$: $Nd_2Mo_2O_7$ and $Nd_2Mo_3O_9$. Stability ranges of all compounds have been determined and are compared to those observed in the neighboring systems. The role of the rare earth element in selective oxidation of molybdenum to oxidation states IV, V, and VI is discussed. Based on the phase equilibria at 1473°K, the standard free energies of formation of Nd_2MoO_5, Nd_3MoO_7, Nd_6MoO_{12}, and Nd_2MoO_6 have been determined. X-ray diffraction data are given for all compounds. Their structural relationship to the homologous compounds formed in the systems with La, Pr, and Sm is discussed.

---

* Author to whom correspondence should be addressed.

0022-4596/81/060294-08$02.00/0

Experimental

1. *Materials*

Starting materials were neodymium sesquioxide (Rhône-Poulenc, 99.9%) and molybdenum powder obtained by reduction in hydrogen at 1273°K of the molybdenum (VI) oxide (Merck, >99.5%). Desired ratios of Nd_2O_3/Mo were mixed in an agate mortar, pressed into pellets and sintered under controlled gaseous atmospheres at 1273, 1473, and 1673°K.

2. *Apparatus and Procedures*

Heating was achieved in an electrical furnace with a temperature control of ±5°C. Control of oxygen pressures was achieved by mixing carbon dioxide and hydrogen in various ratios. The oxygen partial pressure was measured by means of a solid electrolyte cell composed of $(ZrO_2)_{0.85}(CaO)_{0.15}$. The difference between measured and calculated oxygen partial pressures was within ± 0.10 in terms of log p_{O_2} in the range 10^{-5}–10^{-14} atm. The equilibrium between condensed and gaseous phases was reached by oxidation and reduction reactions. After equilibration, the samples were rapidly cooled. Heat treatments extended 3 or 4 days until equilibrium was achieved and at least two heat treatments were performed.

3. *Analysis*

Phases were identified by the powder X-ray diffraction method with a Siemens diffractometer. The oxygen content of the samples after reaction was determined thermogravimetrically and the mean oxidation number of molybdenum deduced.

Lattice parameters of all compounds were calculated from Debye–Scherer diffractograms (calibrated with KCl) using nickel-filtered Cu*Kα* radiation ($\lambda = 1.5405$ Å). Data were refined by least-squares computer program. Reported intensities were derived from relative peak heights.

Results

1. *Phase Equilibria*

Figure 1 shows phase equilibria in the Nd_2O_3–MoO_2–MoO_3 system at 1273°K. Stable phases under the present experimental conditions were found for the molar ratios Nd_2O_3/Mo: 3/1, 5/2, 1/1, and 1/3 corresponding to formulas Nd_6MoO_{12}, $Nd_{10}Mo_2O_{21}$, Nd_2MoO_6, and $Nd_2(MoO_4)_3$ on the pseudobinary line Nd_2O_3–MoO_3, and to formulas Nd_2MoO_5 and $Nd_2Mo_3O_9$ on the pseudobinary line Nd_2O_3–MoO_2. For the ratio 1/1 a molybdenum V + VI compound, $Nd_{12}Mo_6O_{35}$, forms between Nd_2MoO_5 and Nd_2MoO_6. A molybdenum V compound, Nd_3MoO_7, forms for the ratio 3/2 and for the ratio 1/2 a molybdenum V compound with scheelite structure, $NdMoO_4$ has been observed.

Phase equilibria are significantly different at 1473°K. A portion of the phase diagram between 1273 and 1473°K has been published in a preliminary study (*4*). Figure 2 shows that the scheelite phase is no longer stable whereas the molybdenum IV compounds Nd_2MoO_5 and $Nd_2Mo_3O_9$ are still observed. Stability ranges in terms of oxygen partial pressure of the observed compounds at 1273°K and 1473°K are listed in

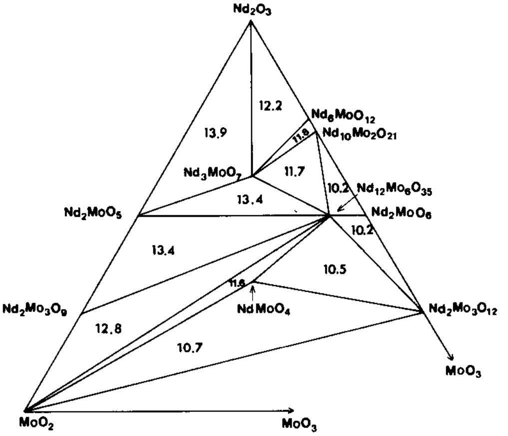

FIG. 1. The Nd_2O_3–MoO_2–MoO_3 isotherm at 1273°K.

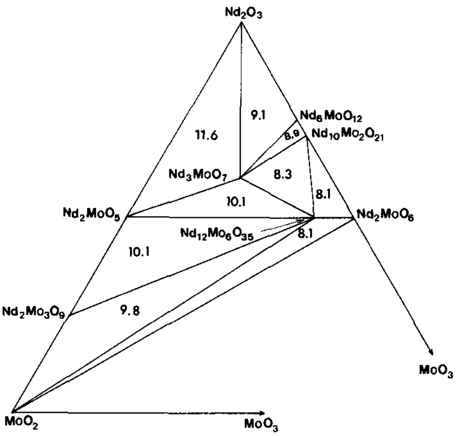

FIG. 2. The Nd_2O_3–MoO_2–MoO_3 isotherm at 1473°K.

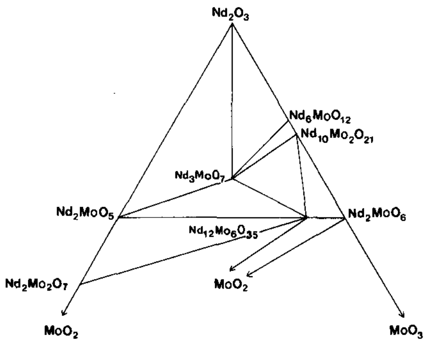

FIG. 3. Portion of the phase diagram of the Nd_2O_3–MoO_2–MoO_3 system at 1673°K.

Table I. Pure neodymium oxide was stable in the pressure range applied: 10^{-5}–10^{-14} atm. Phase relations and stable phases at 1673°K are represented in Fig. 3. The oxygen partial pressures necessary to produce these equilibrium relations have not been determined very precisely at this temperature and are not reported here. The numbers on all figures refer to $-\log p_{O_2}$ (atm) and are given with an accuracy of ±0.1 in terms of $\log p_{O_2}$.

Composition of all phases was deduced from phase equilibria results. In the neodymium-rich portion of the phase diagram, all phases could be prepared as pure compounds. Since rapid oxidation from Mo to MoO_2 takes place even under very low oxygen partial pressures it was more difficult to deduce from isobaric paths the exact composition of the cubic-related phase in the MoO_2-rich portion of the phase diagram. Owing to its very narrow stability range, the scheelite compound could not be obtained as a single phase. However, its powder pattern could be indexed satisfactorily.

2. *Calculations of the Standard Free Energies of Formation of Nd_2MoO_5, Nd_3MoO_7, Nd_6MoO_{12} and Nd_2MoO_6*

On the basis of the present phase equilibria, the following standard free energies of formation have been determined at 1473°K

TABLE I

STABILITY RANGES IN TERMS OF $-\log p_{O_2}$ (atm)

Compound	1273°K		1473°K	
	Lower limit	Upper limit	Lower limit	Upper limit
Nd_6MoO_{12}	12.2	~0.7 (in air)	9.1	~0.7
$Nd_{10}Mo_2O_{21}$	11.8	~0.7	8.9	~0.7
Nd_2MoO_6	10.2	~0.7	8.1	~0.7
$Nd_2(MoO_4)_3$	10.5	~0.7	—	—
Nd_3MoO_7	13.9	11.7	11.6	8.3
$Nd_{12}Mo_6O_{35}$	13.4	10.2	10.1	8.1
$NdMoO_4$	11.6	10.7	—	—
Nd_2MoO_5	>14	13.4	13.8	10.1
$Nd_2Mo_3O_9$	>14	12.8	>13	9.8

from metallic molybdenum, Nd_2O_3, and oxygen:

$$Mo + Nd_2O_3 + O_2 = Nd_2MoO_5 \quad (1)$$

$$Mo + \tfrac{3}{2}Nd_2O_3 + \tfrac{5}{4}O_2 = Nd_3MoO_7 \quad (2)$$

$$Mo + 3Nd_2O_3 + \tfrac{3}{2}O_2 = Nd_6MoO_{12} \quad (3)$$

$$Mo + Nd_2O_3 + \tfrac{3}{2}O_2 = Nd_2MoO_6 \quad (4)$$

The solid compounds of the system being pure phases, their activity is set equal to one in the following calculations.

The equilibrated $\log p_{O_2}$ value connected with Eq. (1) was −13.8 and the standard free energy change referred to Eq. (1), $\Delta G°(1)$, was calculated to be −93.1 kcal/mole of Nd_2MoO_5.

For Nd_3MoO_7 the standard free energy change may be calculated using:

$$Nd_2MoO_5 + \tfrac{1}{2}Nd_2O_3 + \tfrac{1}{4}O_2 = Nd_3MoO_7. \quad (5)$$

The value of $\log p_{O_2}$ related to Eq. (5) was −11.6 and the standard free energy change of Eq. (5), $\Delta G°(5)$, is calculated to be −19.56 kcal/mole of Nd_3MoO_7. Adding $\Delta G°$ (*1*) and $\Delta G°(5)$, the standard free energy of formation of Nd_3MoO_7 referred to Eq. (2), $\Delta G°(2)$, is −112.66 kcal/mole. The lowest oxygen partial pressure at which Nd_6MoO_{12} is in equilibrium with Nd_3MoO_7 is $10^{-9.10}$ atm at 1473°K. The standard free energy change, $\Delta G°(6)$, referred to the following equation is calculated to be −15.33 kcal/mole of Nd_6MoO_{12}:

$$\tfrac{3}{2}Nd_2O_3 + Nd_3MoO_7 + \tfrac{1}{4}O_2 = Nd_6MoO_{12}. \quad (6)$$

By adding $\Delta G°(6)$ and $\Delta G°(2)$, the standard free energy of formation of Nd_6MoO_{12} referred to Eq. (3) is −127.83 kcal/mole.

From phase equilibria, the formation of $Nd_{12}Mo_6O_{35}$ is an intermediate step in the oxidation of Nd_2MoO_5 to Nd_2MoO_6 and the standard free energy change may be calculated using

$$6Nd_2MoO_5 + \tfrac{5}{2}O_2 = Nd_{12}Mo_6O_{35} \quad (7)$$

and

$$\tfrac{1}{6}Nd_{12}Mo_6O_{35} + \tfrac{1}{12}O_2 = Nd_2MoO_6 \quad (8)$$

The value of $\log p_{O_2}$ related to Eq. (7) and (8) was −10.15 and −8.15, respectively; the standard free energy changes related to Eq. (7) and (8) were calculated to be $\Delta G°(7)$ = −171.2 kcal/mole of $Nd_{12}Mo_6O_{35}$, and $\Delta G°(8)$ = −4.58 kcal/mole of Nd_2MoO_6. By adding $\tfrac{1}{6}$ $\Delta G°(7)$, $\Delta G°(8)$, and $\Delta G°(1)$ we obtain the standard free energy of formation of Nd_2MoO_6, $\Delta G°(4)$, referred to Eq. (4), to be −126.21 kcal/mole of Nd_2MoO_6.

3. *Radiocristallographic Analysis*

The binary compounds between Nd_2O_3 and MoO_3 are described first: *Nd_6MoO_{12}* is isostructural with La_6MoO_{12} (*5*) and Pr_6MoO_{12} (*3*) and has the well-known rhombohedrally distorted fluorite structure of Y_6UO_{12} (*6*). The hexagonal cell parameters of the rhombohedral cell are a = 10.246(6) Å and c = 9.672(5) Å with V = 879 $Å^3$ (Table III). The value of c/a = 0.944 is very close to the value of 0.9458 calculated for the "ideal" rhombohedral cell (*8*). At 1673°K, Nd_6MoO_{12} still exhibits rhombohedral symmetry like La_6MoO_{12} and Pr_6MoO_{12}.

$Nd_{10}Mo_2O_{21}$ shows typical fcc-type reflections which give a cell edge of a = 5.520 (3) Å and V = 168 $Å^3$. The patterns at

TABLE II

SUMMARY OF THE STANDARD FREE ENERGY VALUES

Reaction	$\Delta G°$ (kcal/mole)
(1) $Mo + Nd_2O_3 + O_3 = Nd_2MoO_5$	−93.10
(2) $Mo + \tfrac{3}{2}Nd_2O_3 + \tfrac{5}{4}O_2 = Nd_3MoO_7$	−112.66
(3) $Mo + 3\ Nd_2O_3 + \tfrac{3}{2}O_2 = Nd_6MoO_{12}$	−127.83
(4) $Mo + Nd_2O_3 + \tfrac{3}{2}O_2 = Nd_2MoO_6$	−126.21
(5) $Nd_2MoO_5 + \tfrac{1}{2}Nd_2O_3 + \tfrac{1}{4}O_2 = Nd_3MoO_7$	−19.56
(6) $\tfrac{3}{2}Nd_2O_3 + Nd_3MoO_7 + \tfrac{1}{4}O_2 = Nd_6MoO_{12}$	−15.33
(7) $6\ Nd_2MoO_5 + \tfrac{5}{2}O_2 = Nd_{12}Mo_6O_{35}$	−171.20
(8) $\tfrac{1}{6}Nd_{12}Mo_6O_{35} + \tfrac{1}{12}O_2 = Nd_2MoO_6$	−4.58

1273 and 1473°K are cubic. After prolonged heating at 1673°K, a slight broadening of the [200] and [311] lines appears, which is distinct from the $K\alpha_1$–$K\alpha_2$ splitting. This would indicate tetragonal symmetry. At 1673°K one could have a pseudotetragonal cell with $a = b = 5.523$ (3) Å, $c = 5.512$ (3) Å, and $V = 168$ Å^3. The two Mo VI compounds being very close in composition might explain why they have been confused (*9*).

Nd_2MoO_6 (*7*) and *$Nd_2(MoO_4)_3$* (*10, 11*) are well known and will not be described here.

On the pseudobinary line Nd_2O_3–MoO_2, compounds exhibit different structure types according to their composition:

Nd_2MoO_5, which has been described (*1*), is monoclinic like Yb_2ReO_5 with $a = 7.756$ (5) Å, $b = 5.823$ (4) Å, $c = 12.648$ (6) Å, and $\beta = 107.85°$. These values are in good agreement with those published recently by other workers who prepared Nd_2MoO_5 by selective hydrogen reduction of Nd_2MoO_6 at 1148°K (*12, 13*). The monoclinic cell can be related to a cubic fluorite cell as follows:

$$a_M \simeq \sqrt{2} \times a_F,$$

$$b_M \simeq a_F,$$

$$c_M \simeq 4/\sqrt{3} \times a_F \qquad (a_F = 5.5 \text{ Å}).$$

TABLE III

X-Ray Powder Diffraction Data for Nd_6MoO_{12}

$h\ k\ l$	d_{obs}	d_{calc}	I/I_0
0 0 3	3.22	3.22	35
2 1 1	3.167	3.169	100
2 1 2	2.751	2.756	38
2 1 4	1.961	1.961	24
4 1 0	1.937	1.936	23
2 1 5	1.675	1.675	9
4 1 3	1.658	1.660	18
4 2 1	1.651	1.652	11
0 0 6	1.611	1.612	2
4 2 2	1.584	1.584	5
4 2 4	1.378	1.378	4

A relationship to fluorite cell can also be written for tetragonal Nd_2MoO_6: $a_T \simeq 3/4a_F$, $c_T \simeq 3a_F$ ($a_F = 5.3$ Å).

$Nd_2Mo_2O_7$ is a high-temperature phase and forms only above 1473°K. The powder pattern shows very strong pyrochlore-type reflections like $Sm_2Mo_2O_7$, which give a cell edge of $a = 10.437(7)$ Å. However, one weak line could not be indexed in the cubic system (Table IV), indicating that the true symmetry might be lower and orthorhombic or monoclinic like $Nd_2Ti_2O_7$ (*14*) or $Ca_2Nb_2O_7$ (*15*). Actually a single-crystal analysis has been undertaken and will be reported on later.

$Nd_2Mo_3O_9$: Phase equilibria studies show formation of this compound for the ratio $Ln/\text{Mo} = 2/3$ and indicate that it is a molybdenum IV compound. The powder pattern shows very strong body centered cubic reflections (Table V). All reflections could be satisfactorily indexed by doubling the cubic cell edge and introducing a slight tetragonal distortion which led to a tetragonal cell with parameters: $a = b = 21.327(9)$ Å, $c = 21.138(9)$ Å, and $V = 9614(6)$ Å^3.

Finally the three compounds characterized in the ternary system will be described.

The *$NdMoO_4$* phase exists only at 1273°K (Fig. 1) and has been indexed in a tetragonal cell with $a = 5.216(3)$ Å, $c =$

TABLE IV

X-Ray Powder Diffraction Data for $Nd_2Mo_2O_7$

$h\ k\ l$	d_{obs}	d_{calc}	I/I_0
2 2 2	3.010	3.013	100
—	2.864	—	4
4 0 0	2.606	2.609	25
3 3 1	2.391	2.394	4
5 1 1	2.008	2.008	2
4 4 0	1.846	1.845	28
6 2 2	1.572	1.573	22
4 4 4	1.506	1.506	12

TABLE V

X-RAY POWDER DIFFRACTION DATA FOR $Nd_2Mo_3O_9$

$h\ k\ l$	d_{obs}	d_{calc}	I/I_0
3 2 1	5.71	5.69	100
4 4 0	3.774	3.770	42
3 2 6	3.033	3.027	4
6 0 4	2.947	2.949	2
6 4 2	2.850	2.848	71
6 4 4	2.579	2.580	1
2 1 9	2.282	2.280	7
10 5 1	1.901	1.900	10
5 0 11	1.752	1.752	3
11 1 10	1.425	1.425	5

11.44(1) Å, and $V = 311(7)$ Å³. These values are in good agreement with the lattice parameters measured for $SmMoO_4$ (*3*) and the scheelite-type compounds $LnMoO_4$, known for the heavy rare earth elements (Ln = Gd–Lu, Y) (*16*).

$Nd_{12}Mo_6O_{35}$ is a fluorite-type compound with an orthorhombic unit cell derived from single-crystal analysis: a = 10.873(3) Å, b = 5.653(2) Å, c = 27.70(1) Å, and V = 1518(1) Å³ (*2*). The powder pattern consists of very strong fcc-type reflections and a few superstructure lines producing lower symmetry (Table VI).

Nd_3MoO_7 is also fluorite-related and has been indexed in an orthorhombic *c*-centered cell like Nd_3NbO_7 (*17*) with a = 10.804(5) Å, b = 7.505(2) Å, c = 7.603(2) Å, and V = 616 Å³ (Table VII). From these data the orthorhombic cell could be related to a cubic fluorite cell with $b_{orth} \simeq c_{orth} = a_F\sqrt{2}$ and $a_{orth} \simeq 2a_F$ (a_F = 5.38 Å). This new molybdenum V compound has been found isostructural with the homologous niobium V and tantalum V compounds (*18*).

Discussion

Phase equilibria results indicate that the most stable Mo VI compound against reduction is Nd_6MoO_{12}, corresponding to the

TABLE VI

X-RAY POWDER DIFFRACTION DATA FOR $Nd_{12}Mo_6O_{35}$

$h\ k\ l$	d_{obs}	d_{calc}	I/I_0
1 1 5	3.51	3.52	4
1 1 6	3.179	3.182	100
3 1 2	2.962	2.962	4
2 0 7	2.957	2.960	4
0 2 2	2.753	2.755	43
1 1 9	2.408	2.408	4
4 1 2	2.402	2.403	4
3 0 8	2.348	2.350	3
4 1 3	2.345	2.348	3
4 1 5	2.194	2.195	4
3 2 2	2.193	2.193	4
3 0 9	2.189	2.188	4
1 2 7	2.162	2.162	6
4 0 7	2.156	2.153	6
2 2 8	1.947	1.947	62
6 1 4	1.661	1.662	47
6 1 6	1.591	1.591	12
6 1 7	1.549	1.550	4
0 4 4	1.377	1.377	8

TABLE VII

X-RAY POWDER DIFFRACTION DATA FOR Nd_3MoO_7

$h\ k\ l$	d_{obs}	d_{calc}	I/I_0
0 2 1	3.366	3.365	12
2 0 2	3.115	3.109	100
2 2 0	3.086	3.082	86
3 1 1	2.990	2.986	9
2 2 1	2.855	2.856	12
4 0 0	2.704	2.701	15
0 2 2	2.669	2.670	31
3 1 2	2.469	2.469	2
1 3 0	2.437	2.437	2
4 2 1	2.104	2.106	7
5 1 1	2.004	2.003	9
0 0 4	1.901	1.901	43
0 4 0	1.877	1.876	4
5 1 2	1.822	1.822	6
2 4 1	1.726	1.726	7
2 2 4	1.618	1.618	17
2 4 2	1.607	1.606	11
4 0 4	1.554	1.554	7
7 1 1	1.480	1.483	3
2 4 3	1.452	1.452	3

highest ratio *Ln*/Mo. This has also been observed for the systems with Pr and Sm. From the values reported in Table I and the standard free energy values listed in Table II, one notes the small changes in $\Delta G°$ from one compound to the other and the particular stability against reduction of the molybdenum V + VI compound $Nd_{12}Mo_6O_{35}$. Moreover, for all systems in which the fluorite-type phase $Ln_{12}Mo_6O_{35}$ has a large stability domain, isobaric paths show $Ln_2(MoO_4)_3$ to be more stable against reduction than Ln_2MoO_6. The very narrow stability range of the scheelite phase $NdMoO_4$ might explain why it could not be prepared by the evacuated sealed-tube technique as can $LnMoO_4$ (*Ln* = Y, Gd–Lu) (*16*).

The phase diagram observed at 1473°K (Fig. 2) is characteristic for the Pr, Nd, and Sm systems, with the exception that under the experimental conditions no $Ln_{14}Mo_4O_{33}$-type compound has been observed between $Nd_{10}Mo_2O_{21}$ and Nd_2MoO_6. However, stabilization against reduction depends essentially upon the nature and the size of the rare earth ion: the larger the ionic radius, the more molybdenum, in a given oxidation state, is stabilized toward low oxygen partial pressures.

The size of the rare earth cation determines also the structure type of the ternary compounds.

From La to Nd, the fluorite-structure-related compounds, Ln_6MoO_{12} are rhombohedral, then cubic from Sm to Ho (*3*) and again rhombohedral from Er to Lu (*19*). It should be noted that for the tungstates, Ln_6WO_{12}, different structural classes have been found, depending on the size of the Ln^{3+} element (*20*).

$Nd_{10}Mo_2O_{21}$ is of fcc type, like $Pr_{10}Mo_2O_{21}$ and $Sm_{10}Mo_2O_{21}$. Compounds of this formula have been found from La to Tb. Allowing for the shifts in interplanar spacings due to the lanthanide contraction, one sees that the $Ln_{10}Mo_2O_{21}$ X-ray patterns are in fact identical to those of the cubic Ln_6MoO_{12} compounds (Sm to Tb) but experiments show no evidence of a solid solution between Ln_6MoO_{12} and $Ln_{10}Mo_2O_{21}$.

The molybdenum V compounds, Ln_3MoO_7, also related to the fluorite structure are orthorhombic for La and Pr to Eu (*3*). For the heavier lanthanides, the temperature of formation gradually increases (>1473°K for Gd_3MoO_7, ~1673°K for Tb_3MoO_7) and the compounds exhibit a defect fluorite-type structure. Investigations on these new compounds will be published separately.

$Nd_2Mo_3O_9$ is isostructural with $Sm_2Mo_3O_9$ and occurs from Nd to Tb (*3*). The compound forms between 1273 and 1473°K, but has not been observed at 1673°K. As has been pointed out (*3*), the strong body-centered-cubic reflections (Table V) might indicate a structural relationship to the cubic $KSbO_3$-type compounds which form for the same ratio Ln/M = 2/3, like $La_4Re_6O_{19}$ (*21*) and isostructural compounds with *M* = Ru, Os (*22*). Moreover, the structure of these $La_4Re_6O_{19}$-type phases is characterized by very short Re–Re distances indicating metal–metal bonding. Many of the molybdenum IV compounds which have been investigated show also Mo–Mo bonding as in MoO_2, $M_2Mo_3O_8$ (*23*), and Ln_2MoO_5 (*1*).

References

1. H. Kerner-Czeskleba and G. Tourne, *Mater. Res. Bull.* **13**, 271 (1978).
2. H. Kerner-Czeskleba and B. Cros, *Mater. Res. Bull.* **13**, 947 (1978).
3. H. Kerner-Czeskleba, Third International Conference on the Chemistry and Uses of Molybdenum, Ann Arbor, August 19–23, 1979.
4. H. Kerner-Czeskleba, *C.R. Acad. Sci. Paris Ser. C* **287**, 369 (1978).
5. B. Cros and H. Kerner-Czeskleba, *Rev. Chim. Miner.* **15**, 521 (1978).

6. S. F. Bartram, *Inorg. Chem.*, **5**, 749 (1966).
7. L. H. Brixner, A. W. Sleight, and M. S. Licis, *J. Solid State Chem.* **5**, 186 (1972).
8. D. Michel, A. Kahn, and M. Perez y Jorba, *Mater. Res. Bull.* **11**, 857 (1976).
9. J. P. Fournier, J. Fournier, and R. Kohlmuller, *Bull. Soc. Chim. Fr.* **12**, 4277 (1970).
10. K. Nassau, J. W. Shiever, and E. T. Keve, *J. Solid State Chem.* **3**, 411 (1971).
11. L. H. Brixner, A. W. Sleight, and M. S. Licis, *J. Solid State Chem.* **5**, 247 (1972).
12. A. Manthiram and J. Gopalakrishnan, *Proc. Indian Nat. Sci. Acad. Sect. A* **87**(8), 267 (1978).
13. A. Manthiram and J. Gopalakrishnan, *J. Less-Common Metals* **68**, 167 (1979).
14. K. Scheunemann and H. K. Muller-Buschbaum, *J. Inorg. Nucl. Chem.* **37**, 2261 (1975).
15. N. Ishizawa, F. Marumo, S. Iwai, M. Kimura, and T. Kawamura, *Acta Crystallogr. Sect. B* **36**, 763 (1980).
16. E. Banks and M. Nemiroff, *Inorg. Chem.* **13**, 2715 (1974).
17. J. G. Allpress and H. J. Rossell, *J. Solid State Chem.* **27**, 105 (1979).
18. H. J. Rossell, *J. Solid State Chem.* **27**, 115 (1979).
19. E. A. Aitken, S. F. Bartram and E. F. Juenke, *Inorg. Chem.* **5**, 949 (1964).
20. G. J. McCarthy, R. D. Fisher, G. G. Johnson, and C. E. Gooden, 5th Material Research Symposium on Solid State Chemistry, Washington, D.C., October 1971.
21. N. L. Morrow and L. Katz, *Acta Crystallogr. Sect. B* **24**, 1466 (1968).
22. F. Abraham, J. Trehoux, and D. Thomas, *Mater. Res. Bull.* **12**, 43 (1977).
23. D. Bertrand and H. Kerner-Czeskleba, *J. Phys.* **36**, 379 (1975).